© The American Society of Gene Therapy

Functional Cone Rescue by RdCVF Protein in a Dominant Model of Retinitis Pigmentosa

Ying Yang[1,2], Saddek Mohand-Said[1–3], Aude Danan[3], Manuel Simonutti[1,2], Valérie Fontaine[1,2], Emmanuelle Clerin[1,2], Serge Picaud[1,2], Thierry Léveillard[1,2] and José-Alain Sahel[1–5]

[1]Université Pierre et Marie Curie-Paris6, UMR-S 592, Paris, France; [2]Institut de la Vision, Institut National de la Santé et de la Recherche Médicale, Paris, France; [3]Centre Hospitalier National d'Ophtalmologie des Quinze-Vingts, service du Pr Sahel, Paris, France; [4]Institute of Ophthalmology, University College of London, London, UK; [5]Fondation Ophtalmologique Adolphe de Rothschild, Paris, France

In retinitis pigmentosa (RP), a majority of causative mutations affect genes solely expressed in rods; however, cone degeneration inevitably follows rod cell loss. Following transplantation and *in vitro* studies, we demonstrated the role of photoreceptor cell paracrine interactions and identified a Rod-derived Cone Viability Factor (RdCVF), which increases cone survival. In order to establish the clinical relevance of such mechanism, we assessed the functional benefit afforded by the injection of this factor in a frequent type of rhodopsin mutation, the P23H rat. In this model of autosomal dominant RP, RdCVF expression decreases in parallel with primary rod degeneration, which is followed by cone loss. RdCVF protein injections induced an increase in cone cell number and, more important, a further increase in the corresponding electroretinogram (ERG). These results indicate that RdCVF can not only rescue cones but also preserve significantly their function. Interestingly, the higher amplitude of the functional versus the survival effect of RdCVF on cones indicates that RdCVF is acting more directly on cone function. The demonstration at the functional level of the therapeutic potential of RdCVF in the most frequent of dominant RP mutations paves the way toward the use of RdCVF for preserving central vision in many RP patients.

Received 11 September 2008; accepted 23 January 2009; published online 10 March 2009. doi:10.1038/mt.2009.28

INTRODUCTION

Retinitis Pigmentosa (RP) is a photoreceptor-degenerative disease caused by various mutations affecting many different genes.[1] Whereas most causative genes are selectively expressed in rod photoreceptors,[2,3] a sequential rod-cone photoreceptor loss is observed in humans as well as in animal models, which is reflected by the designation of this condition as a rod-cone dystrophy. In clinical terms, while the loss of the rod photoreceptors leads to dark-adapted vision loss, the most feared visual impairment is the consequence of the secondary cone photoreceptor loss, as this cell population is necessary for diurnal vision, including photopic visual field, visual acuity, color perception, and contrast sensitivity.[4] Therefore, the development of therapeutic strategies targeting the mechanisms underlying the secondary cone cell death in RP represents a very promising approach. This could be applied in a wide range of mutations expressed in rods, even at late stages of the disease as it has been shown that vision may remain substantial even when 95% of cones have been lost.[5] In other words, keeping the functional cones alive may prevent up to 1.5 million people worldwide becoming blind.[6]

We previously studied the rod-cone cellular interactions and proposed following photoreceptor transplantation studies in the *rd1* mouse that the secondary cone degeneration could be significantly diminished by a surviving signal, released by rods or requiring their presence.[7,8] We subsequently demonstrated *in vitro* that these rod–cone interactions are mediated by secreted proteins.[9,10] A systematic expression-cloning strategy then enabled us to isolate a Rod-derived Cone Viability Factor (RdCVF) encoded by the *Nxnl1 (Txnl6)* gene.[11] This factor is able to rescue cone photoreceptors in the *rd1* mouse. We could not assess the functionality of the rescued cones as at the age of RdCVF injection; that is, once rods had degenerated, the *rd1* mouse no longer presented a measurable electroretinogram (ERG).[12]

In order to validate the therapeutic interest of RdCVF in RP, we performed this study aimed at demonstrating its functional benefit. We have selected a larger animal model carrying a prevalent *RP* gene mutation, the transgenic rhodopsin P23H mutant rat. This corresponds to the most frequent autosomal dominant human RP mutation observed in 12% of autosomal dominant patients in the United States,[1] while the *rd1* mouse is affected by a mutation in the rod-specific β-subunit gene of the cyclic guanosine monophosphate-dependent phosphodiesterase 6,[13] responsible for <5% of autosomal-recessive RP in humans.

We characterized the course of cone photoreceptor degeneration in the P23H rat at both electrophysiological and histological levels and assessed these parameters following RdCVF protein injection. The study provides the first evidence for a functional rescue of cone photoreceptor following RdCVF administration in an animal model of RP. Moreover, our results support a possible role of RdCVF in the maintenance of the functionality of cones.[14]

The clinical significance of such functional rescue cannot be underestimated, in view of the reported discrepancy between

The first two authors contributed equally to this work.

Correspondence: *Thierry Léveillard, Université Pierre et Marie Curie-Paris6, UMR-S 592, Paris, F-75012 France. E-mail: thierry.leveillard@inserm.fr*

© The American Society of Gene Therapy

the morphological and functional effects on photoreceptor cells of another neuroprotective agent,[15] ciliary neurotrophic factor, currently in phase II clinical trials.[16]

RESULTS

Secondary cone loss follows rod cell death in the P23H transgenic rats

In the P23H rat model, a transgene corresponding to the P23H mutated mouse rhodopsin gene is expressed under the control of the rhodopsin promoter and thus expressed selectively by rod photoreceptors.[17] Histology sections show progressive thinning and loss of outer segments and outer nuclear layer between 2 and 8 months corresponding to rod loss in the heterozygotous P23H rats as previously published (ref. 18, data not shown). **Figure 1a** shows the decrease of cone density, estimated by stereological cell counting from 3 to 9 months. By 6 months of age most rods have degenerated, while only 41% of cones have been lost with a further 28% loss of cones between 6 and 9 months.

Functional assessment performed by ERG recordings shows a loss of scotopic and photopic function during photoreceptor degeneration (**Figure 1b–e**). The average amplitude of the scotopic ERG B-wave was reduced by 75% between 2 and 4 months (from 268 to 66 µV; **Figure 1d** and **Table 1**) and was further reduced by up to 89% at 9 months (29 µV), while the photopic ERG B-wave amplitude decreased by 56% (77 µV versus 34 µV) and 77% (18 µV), respectively, during the same periods. Loss of cone function was further confirmed by flicker ERG (**Figure 1e**).

Thus, as observed for the *rd1* mouse,[9,11,19] rod degeneration, triggered here by the expression of the mutant protein in rod cells, is followed by a secondary loss of cones through a noncell-autonomous mechanism. The sequential degeneration of rods and cones in the heterozygotous P23H model, therefore, makes it an appropriate model for the assessment of cone-rescue strategies.

Decreased RdCVF expression correlates with rod loss in the P23H rat model

We then investigated the expression of RdCVF, a trophic factor expressed in a rod-dependent manner in the mouse.[11] Mouse RdCVF-L protein sequence (Uniprot: Q8VC33) was used to identify the rat RdCVF sequence (**Figure 2a,b**). As for the mouse *Nxnl1* (*Txnl6*) and *Nxnl2* genes, different forms of RdCVF mRNAs were identified resulting most likely from alternative splicing.[20] Using reverse transcription (RT-PCR), RdCVF-Total expression (short and long forms) was found to be expressed in the neural retina but not in the retinal pigment epithelium of the rat (**Figure 3a**). Using specific primers, we quantified by real-time RT-PCR the expression of RdCVF and RdCVF-L mRNAs. The steady-state level of RdCVF total mRNAs increased gradually during the period from PN10 to PN30 in wild-type retinas; however, in P23H retinas it reached a maximum expression at PN20 (lower than that in wild-type retinas at this stage) and then decreased by PN30 (**Figure 3b**). β-Actin was used as an internal control and the relative expression of RdCVF was 27 and 7% in the Sprague-Dawley and Pro23His rat retinas, respectively; they represent only 1.1 and 0.8% in the P23H rat retina at 6 months of age, after rod photoreceptors have been lost. Quantitative RT-PCR also shows a rod-dependent expression matching that of rod

Table 1 Scotopic and photopic ERG amplitude and latency of Sprague-Dawley and P23H rats

	Scotopic B wave (1 log cd/m²)		Photopic B wave (1.4 log cd/m²)	
	Latency (ms)	Amplitude (µV)	Latency (ms)	Amplitude (µV)
Sprague-Dawley ($N = 12$)	81 ± 8	913 ± 165	68 ± 12	201 ± 63
P23H 2 months	85 ± 13	268 ± 34 CI: 248–287	67 ± 16	77 ± 19 CI: 66–88
P23H 4 months	96 ± 12	66 ± 16 CI: 57–75	96 ± 13	34 ± 9 CI: 28–41
P23H 6 months	98 ± 12	45 ± 19 CI: 35–54	96 ± 11	28 ± 16 CI: 20–36
P23H 9 months	105 ± 20	29 ± 16 CI: 23–35	105 ± 23	18 ± 13 CI: 15–22

CI: 95% confidence interval, which is an interval estimate of a population parameter. Here are shown only the confidence intervals of P23H rat electroretinogram (ERG) scotopic and photopic B wave amplitude from 2 to 9 months.
cd, candela.

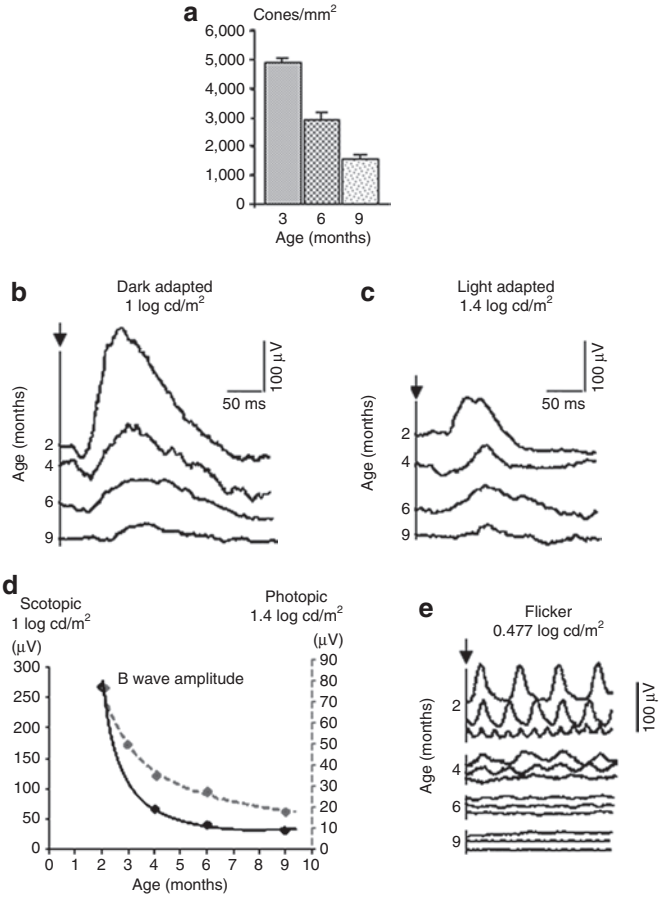

Figure 1 Photoreceptor degeneration of P23H mutant rats. (**a**) Cone counts: 3 months: 4,913 ± 128 c/mm²; 6 months: 2,894 ± 259 c/mm²; and 9 months: 1,527 ± 166 c/mm². (**b**) Mixed responses to single flashes of intensity [1 log candela (cd)/m²] in dark adapted condition of P23H rats at different ages. (**c**) Under photopic adaptation, responses to single flashes (1.4 log cd/m²) of P23H rats at different ages. (**d**) Curved lines display scotopic (solid line) and photopic (broken line) B-wave amplitude reduction with age. (**e**) Under photopic adaptation, rapid responses of P23H rat retinas to flashes (0.477 log cd/m²) at 10, 20, 30 Hz, showing progressive decreases in Flicker electroretinogram with age.

© The American Society of Gene Therapy

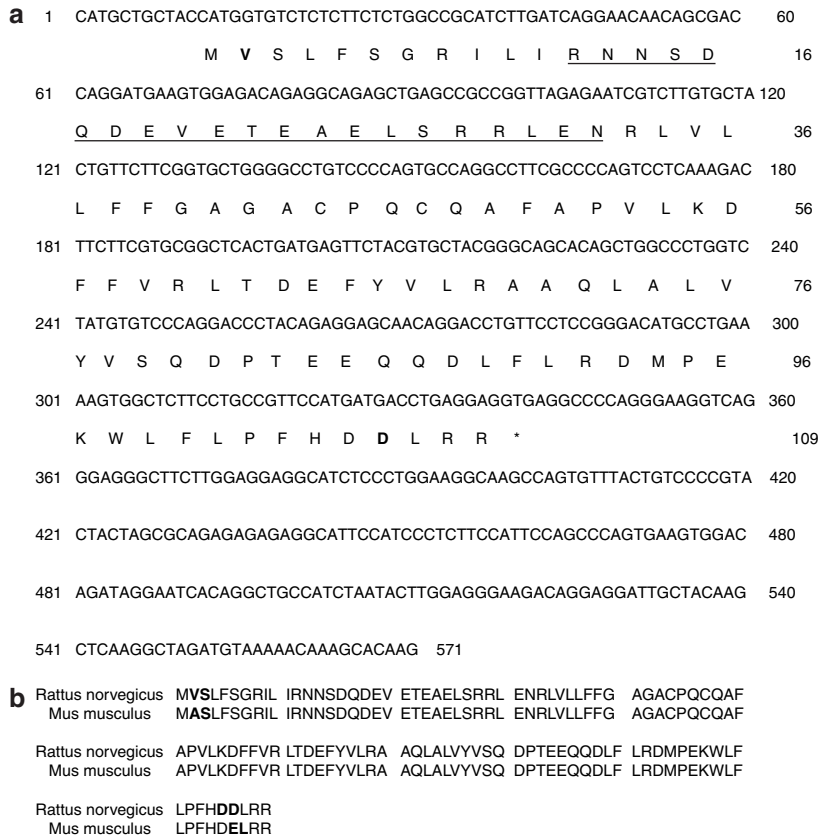

Figure 2 RdCVF-S (short-form) sequence of Rattus norvegicus. (**a**) RdCVF-S nucleotide sequenced and its deduced amino acids sequence. The epitope of the polyclonal antibodies used is underlined. Difference in nucleotide sequence between the two species highlighted in boldface. (**b**) Alignment of rat with mouse RdCVF protein. The amino acid differences between the two polypeptides highlighted in boldface. RdCVF, Rod-derived Cone Viability Factor.

arrestin (data not shown). To confirm the rod-dependent expression of RdCVF, we analyzed by western blotting the expression of RdCVF during the course of rod photoreceptor maturation and degeneration in the P23H rat retina using RdCVF-N rabbit polyclonal antibodies.[11] The intensity of the band corresponding to RdCVF-L is shown to increase during the maturation of the retina between PN10 and 3 months in the wild-type rat, but only up to 2 months in the P23H rat (**Figure 3c**). For the P23H retina the RdCVF-L expression lags behind that of normal retina and starts to decrease from 2.5 to 4 months, which is the period of rod loss. The reduced RdCVF-L immunoreactivity in wild-type retina is most likely reflecting a loading difference as seen on the top panel. A nonspecific band migrating at the position of the short isoform of RdCVF interferes with quantitative analysis. However, in spite of this, a decrease in expression could still be seen at 4 months. We next localized RdCVF expression in the retina by immunohistochemistry using the same antibodies (**Supplementary Materials and Methods**). The expression of the *Nxnl1* (*Txnl6*) gene products could be detected in the Sprague-Dawley rat retina at PN10 with increasing expression to 3 months at which stage stable expression is achieved up to 5 months of age (**Figure 3d**). This expression pattern matches that of rhodopsin in the rod outer segments at the same period. Also, in P23H rat retina, RdCVF labeling is localized to the photoreceptor outer segments, but decreases as the segments shorten (3–5 months).

Subretinal injections of RdCVF protein delay both cone cell death and photopic visual loss

RdCVF protein (109 amino acids) was chemically synthesized (>90% purity) and refolded (**Figure 4a**). The activity of the synthesized protein was measured using an *in vitro* cone-enriched culture system. Just as in the case of a fusion protein purified after expression in *Escherichia coli*, the synthesized protein showed not only equivalent protective activity but also higher purity, with the latter chosen for injection (**Figure 4b**, data not shown) as a result. Three injections of the synthesized polypeptide (1.5 µg) were performed at different time points (separately at the age of 6, 7, 8 month) in the subretinal space of the P23H rats. Phosphate buffered saline was injected as negative control (SM). The cone density in the RdCVF-injected eyes (1,790 ± 231 c/mm^2) at 9 months of age, 1 month after the last subretinal injection, was increased by 19% compared to the sham controls (1,498 ± 141 c/mm^2) and by 20% compared to the contralateral controls (1,497 ± 133 c/mm^2, **Figure 4c**, **Supplementary Tables S1** and **S2**). Moreover, the surviving cones distributed in the whole retina, not only localized in the areas of injection (data not shown).

We also examined the effect of RdCVF injection on cone function by measuring the photopic ERG. An example of the photopic ERG response following RdCVF injections is provided in **Figure 4d**. RdCVF injections were found to limit the decrease in photopic ERG observed between 4 and 9 months (see **Figure 1d**).

© The American Society of Gene Therapy

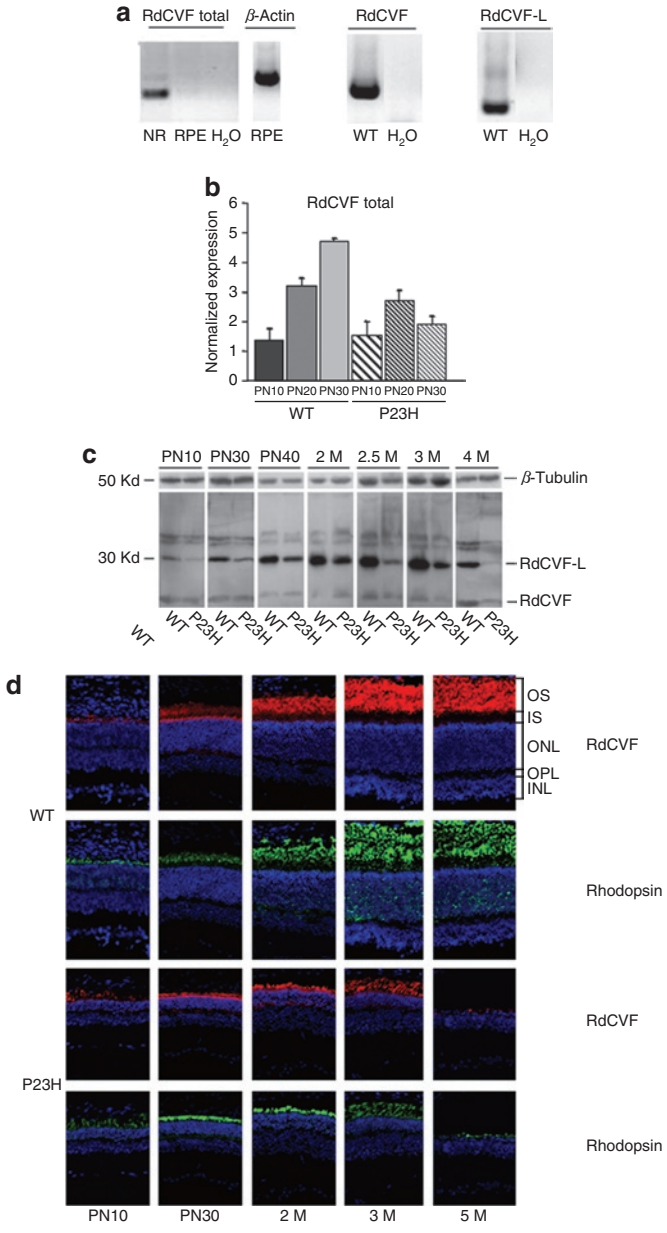

Figure 3 Decreased expression of RdCVF in the P23H retina. (**a**) Reverse transcription (RT)-PCR products of RdCVF-total mRNA amplification from wild-type (WT) rats. β-Actin mRNA by RPE was shown as a positive control. The expression of RdCVF and RdCVF-L mRNA was tested by RT-PCR with specific primer sets. (**b**) Expression of RdCVF total (RdCVF and RdCVF-L) mRNAs in P23H and WT retinas from PN10 to PN30. Results are expressed as a fold difference relative to expression in the RPE taken as reference. Indeed, expression of retinal genes is very low in the RPE and could be considered as background noise. (**c**) Expression of RdCVF protein according to retinal degeneration. Western blotting of protein extracted (40 µg/lane) from P23H and WT retinas [at PN10, 30, 40, and month (M) 2, 2.5, 3, and 4] were probed with anti-RdCVF-N and anti-α-tubulin antibodies. Bands at 50 kd (β-tubulin) and at 30 kd correspond to RdCVF-L protein. β-Tubulin was used to control equal quantities that were loaded in each lane. (**d**) Immunocytochemical localization of RdCVF (red), rhodopsin (green), and 4′,6-diamidino-2-phenylindole (blue) for WT and P23H rats with retinal development. H_2O, no RNA; INL, inner nuclear layer; IS, inner segments; NR, neural retina; ONL, outer nuclear layer; OPL, outer plexiform layer; OS, outer segments; RdCVF, Rod-derived Cone Viability Factor; RPE, retinal pigment epithelium.

The amplitude of the photopic ERG B-wave in RdCVF-injected eyes (**Figure 4e, Supplementary Tables S1** and **S2**, 43 ± 24 µV) was 115 and 126% higher, respectively, than in the contralateral control eyes (20 ± 13 µV) and sham-operated eyes (19 ± 11 µV). The differences observed after RdCVF injection were statistically significant ($P < 0.01$). The scotopic responses, however, did not show any significant difference between all the groups examined. Thus, RdCVF protein administration is providing a selective protection of cone photoreceptor function.

The observation of a larger functional effect, as compared to cytoprotection (**Figure 4e** versus **Figure 4c**) led us to analyze the morphology of photoreceptors. Several reports document that changes in the length and morphology of outer segments occur prior to cell death and that they relate to functional alterations.[21,22] The cones of wild-type retina (**Figure 5a**) displayed longer outer segments than those of P23H rat retina at 9 months of age (**Figure 5b**). The region surrounded by a white line with higher magnification corresponds to the diameter of the tip areas of cone outer segments on flat-mounted retinas. The tip areas of cone outer segments in P23H rat retina (**Figure 5b**) were larger than in wild-type retina (**Figure 5a**). Such shortening of cone outer segments and the enlargement of the tip of cone outer segments on flat-mounted retinas imply that the P23H cones are dysmorphic, which relates to dysfunction even before dying. As the enlargement of the tip of cone outer segments appears as a proper marker of this event, we compared the size of the tip area of cone outer segments from RdCVF-treated, untreated control, and sham-operated retinas. We scanned the flat-mounted RdCVF-injected retinas (9 months of age) stained by peanut agglutinin lectin using an automated acquisition system (**Figure 5c,d**). The measure was performed for five retinas of each group in 40 fields at 0.2 mm from the optic nerve in all directions. The areas of 5–25 cones in each field were measured in a masked test. In **Figure 5i** and **Table 2**, the tip areas of cone outer segments in the RdCVF-treated retinas (21 ± 7 µm²) are 38 and 34% smaller, respectively, than in the untreated control retinas (34 ± 10 µm²) and sham retinas (32 ± 9 µm²). These differences after RdCVF injection were statistically significant (both had same P values; $P < 0.001$). The correlation between cone outer segment morphology and cone function is even more apparent when the data of **Figure 5i** are plotted with those of **Figure 4e**, the data points then align in a strength lane with a regression R of 0.8939. To get more details on the morphology of the cones, the images acquired from nine focus plans were reconstructed in 3D using Metamorph software and converted into 2D using the optimal focus as shown in **Figure 5e,f**. The surface of the selected cells is 6.6 µm² (**Figure 5e**), 4.5 µm² (**Figure 5f**). The hollow area inside is 1.9 µm² (**Figure 5e**), 0.8 µm² (**Figure 5f**). These data imply that the total surface of the selected cell and the inner hole area are smaller in RdCVF-treated P23H retina than in untreated control P23H retina. Furthermore, we scanned the cone cells from both the RdCVF-treated and nontreated retinas by using confocal microscope and we observed smaller ellipse tip area (white star) and longer outer segment in the RdCVF-treated retina (double arrow in **Figure 5h, Supplementary Figure S1**), than in the nontreated retina (**Figure 5g, Supplementary Figure S1**). Therefore, RdCVF injection induced a morphological pattern resembling that observed in normal cones or prior to rod degeneration. This

© The American Society of Gene Therapy

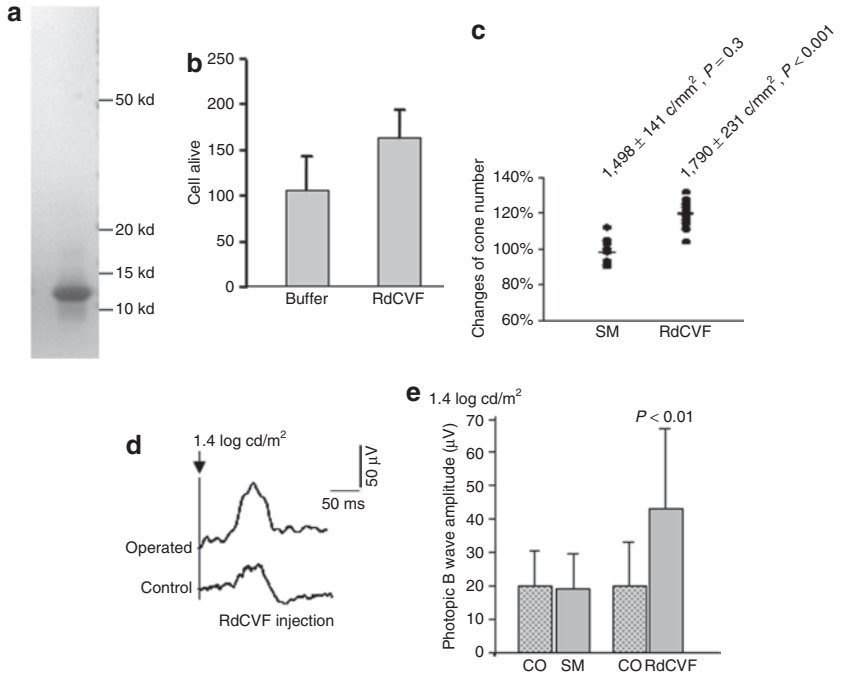

Figure 4 Effect of RdCVF peptide injection to P23H retinas at 9 months of age. (**a**) Coomassie staining of the synthetic RdCVF protein. (**b**) Protective effect of the RdCVF synthetic protein of the cone-enriched cultures from chicken embryos. (**c**) Percentage of changing cone number by normalization from the injected and corresponding control eyes. (SM: 98%, RdCVF: 120%, $^{**}P < 0.001$). (**d**) Comparison of photopic electroretinogram (ERG) average of five single flashes from a P23H rat (B-wave amplitude: control eye = 36 µV, operated eye = 83 µV). (**e**) Amplitudes of photopic ERG B-wave of the treated and control eyes in each group. CO, control eye; SM, sham control eye; RdCVF, Rod-derived Cone Viability Factor-injected eye.

observation that the morphology of cone outer segments after RdCVF injection might be correlated with the increased response to light stimuli is scored in **Figure 4e**.

DISCUSSION

The importance of rod–cone interactions for cone survival was suggested subsequent to the identification of the first causal mutations in RP.[23,24] Indeed, despite the fact that these causal genes are often solely expressed in rods, the degeneration of cones is nonetheless triggered.[19,25,26] The production of animal models with the selective ablation of rod photoreceptors confirmed this rod dependence of cone survival.[27] The rod dependence of cone survival is also supported by the experiments *in vitro*[28] and by the studies of transgenic mice and mutant zebrafish,[29–31] suggesting cell-to-cell interactions in photoreceptor degeneration. Photoreceptor transplantation in the *rd1* mouse provided evidence that rod presence is required for cone survival.[8] The demonstration of the rod–cone dependence was directly provided by coculture experiments.[9] These results were obtained by transplantation and coculture in the *rd1* mouse. Yet this model has important limitations as rods degenerate before the complete differentiation of the photoreceptors. Moreover, cone degeneration is observed at an age when no cone ERG signal can be recorded.[12] We have here used a rat model of RP in another species, the P23H transgenic rat, widely acknowledged as relevant for preclinical studies.

RdCVF was isolated for its effect on cone survival using embryonic chick cone cultures.[11] In the P23H rat retina, by 6 months of age, most rods have degenerated and lost most of their function (**Figure 1b,d**). The effect of the injections of RdCVF protein from 6 to 8 months indicates that this factor induces cone survival directly but does not act indirectly by stimulating rod survival, as most rods have already degenerated at the time of treatment. Similarly, this trophic effect appears independent from the mechanisms of rod degeneration and thus of the causal mutation when the mutated gene is only expressed in rods. Indeed, although photoreceptors undergo apoptosis in both the *rd1* mouse[32] and the P23H rat,[1] this apoptosis is attributed to the cyclic guanosine monophosphate toxicity[33] and Ca^{2+} fluxes in the *rd1* mouse,[34,35] whereas, by contrast, in the P23H model, it is reported to result from a gain of function due to the toxicity of the mutated rhodopsin.[36] Therefore, RdCVF is very likely to act directly on cone survival but not to interfere with the mechanisms of rod degeneration. Furthermore, we also observed that cone photoreceptor distribution extended through the whole retina, but not localized in some areas, showing such an extent of the rescue may relate to the multiple subretinal injections and the spread achieved.

More important, RdCVF induces also a functional rescue, thus validating the potential of this trophic factor for therapeutic applications. On account of the large variance observed in ERGs between rats at the same age, we performed a paired Student's *t*-test for statistical analysis from each rat between the treated and untreated control eyes. On average, the cone numbers were increased by 20% and photopic ERG B-wave amplitudes were increased by 115%. In addition, by comparison between these P23H rats and wild-type rats (201 ± 63 µV), we observed that photopic ERG B-wave amplitudes from the RdCVF protein–injected eyes reached 43% of wild type in contrast to only 10% in the noninjected eyes. The more evident improvement in the ERG

© The American Society of Gene Therapy

measurement compared to overall cone number may indicate that the ratio of functional cones with respect to surviving cones was increased by RdCVF protein injection, implying that RdCVF has a direct effect on cone function. Moreover, ERG B-wave amplitude was ~30 μV when RdCVF injections were started (6 months), then it raised to over 40 μV ($P < 0.01$) after repeated treatment, implying that this improvement might be due to changes in photoreceptor activity, changes in bipolar or horizontal cell function to photoreceptor input, or synaptic connectivity from the surviving cone. We suggest that it might be caused by changes of cone photoreceptor outer segments which were observed both in the photoreceptor transplanted and injected retinas. Recently, it has been shown that exposing the P23H rat for 1 week to photopic ambient light results in the reduction of the cone B-wave amplitude by 57%, an effect that could not be explained by photoreceptor loss as the cone cell density was unchanged and was, however, associated with the shortening of cone outer segments.[37] In addition, the cone outer segments were swollen, delaminated, and vesiculated. Interestingly, after 5 weeks in scotopic conditions the cone B-wave amplitude recovered to 87%, whereas cone outer segments were reorganized and retrieved their elongated morphology. This demonstrates the capacity of cones to recover morphologically and functionally after photooxidative damage and that functional changes are better correlated with cone outer segment morphology than with cone cell density. Furthermore, it has been demonstrated that RdCVF, which is homologous to the thioredoxin family is able to protect cone cells against light irradiation.[38] Correlations between photoreceptor outer segment morphology and ERG were also demonstrated[14] reporting that ciliary neurotrophic factor treatment after 6 days caused a shortening of rod outer segments and a suppression of ERG responses, and all these changes were fully reversible after 3 weeks. They found a 62% reduction in A-wave amplitude, approximately proportional to a 46% reduction in rod outer segment length. With the loss of rod photoreceptors and resulting deficiency of RdCVF in P23H rats, even a high number of cones at the 3-month stage will nevertheless yield a lower ERG photopic B-wave recording (amplitude: 40–50 μV). This indicates that the sequence of events involves first a loss of the function followed by death of photoreceptors. It is known that cones are robust conical-shaped structures that have their cell bodies situated in a single row just below the outer limiting membrane and their inner and outer segments protruding into the subretinal space.[39] We suggest that the increase in diameter of the tip sheath is associated with the shortening of cone outer segments. Our results indirectly indicate a shortening of cone outer segments in the untreated control and sham control retinas. More important, they also indicate that, after RdCVF protein was injected subretinally at 6, 7, and 8 months to the P23H rats, cone outer segments of RdCVF-treated retinas presented a morphological pattern different from their untreated control and sham retinas, as the diameter of the tip sheath was significantly less enlarged, implying partial reversion of changes of cone outer segments. The outer segment is a structure filled entirely with discs

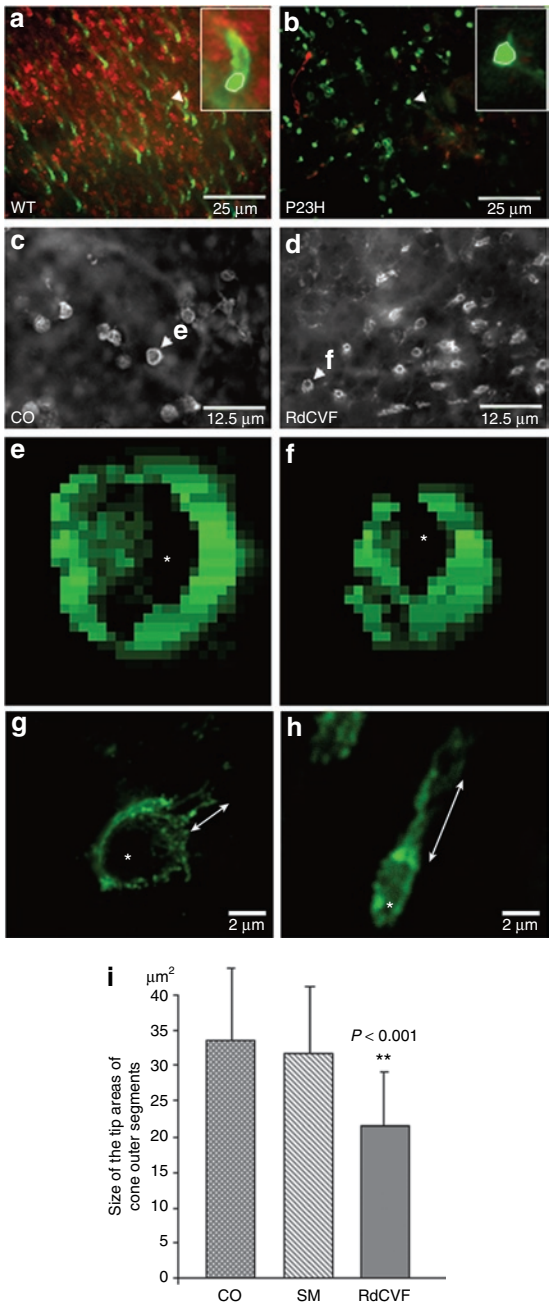

Figure 5 Analysis of the morphology of the cones. (**a,b**) Immunolabeling of PNA lectin (green) and antirhodopsin antibody (red) in **a** wild-type (WT) retina and in **b** P23H retina at 9 months. The cones in the enlarged images (rectangles in the right side of both images **a** and **b**) shown by white arrow head demonstrate that the cone outer segments are longer and the tip areas of cone outer segments (white ellipse line) are smaller in WT retina than in P23H retina. Scale bar = 25 μm. (**c–f**) Automated acquisition system with a marker of PNA lectin displays the tip areas of cone outer segments, which are bigger in **c** the control (CO) than in **d** the RdCVF-treated retina. Scale bar = 12.5 μm. (**e,f**) Using Metamorph software, the cones shown by white arrow head in **e** and **f** were reconstructed in 2D by the optimal focus. The surface of the selected cells is 6.6 μm² (**e**), 4.5 μm² (**f**). The inner hole area (white star) of the selected cells is 1.9 μm² (**e**), 0.8 μm² (**f**). (**g,h**) Two cones scanned by confocal microscope display smaller ellipse tip area (white star) and longer outer segment in **h** the RdCVF-treated retina (double arrow), but not in **g** the nontreated retina. Scale bar = 2 μm. (**i**) Comparison of the tip areas of cone outer segments by PNA labeling in control, sham, and RdCVF-injected retinas. This was performed by analyzing an average of 432 cones per retina. PNA, peanut agglutinin lectin; RdCVF, Rod-derived Cone Viability Factor.

© The American Society of Gene Therapy

Table 2 The size of the tip areas of cone outer segments

Number of the retinas	RdCVF (μm²)	Control (μm²)	Sham (μm²)
1	22.15 ± 6.93	31.03 ± 8.56	35.05 ± 8.31
2	20.72 ± 6.68	31.39 ± 10.28	31.73 ± 10.28
3	25.04 ± 8.25	34.02 ± 9.11	31.02 ± 8.17
4	19.29 ± 6.49	30.77 ± 8.17	29.22 ± 7.68
5	22.16 ± 6.74	39.67 ± 10.43	35.92 ± 10.93
Average of five retinas	21.45 ± 7.21	33.56 ± 9.95	31.81 ± 9.11

RdCVF, Rod-derived Cone Viability Factor.

of folded double membranes in which the light-sensitive visual pigment molecules are embedded; thus, the changes in cone outer segments of surviving cones and the improvement of ERG B-wave amplitude imply that RdCVF actually restores photopic responses in addition to slowing down cone death.

For the treatment of patients with RP, the large number of genes, and, in particular, the dominant inheritance of many types of RP is a major challenge for corrective gene therapy.[40] The neuroprotective effect of fibroblast growth factor-2 in a rat model of inherited retinal dystrophy[41] initiated the search for the most potent protective factors, an approach that would offer therapeutic potential regardless of the causal mutation. Ciliary neurotrophic factor is currently being evaluated in a clinical trial,[15] although the paradoxical decrease in both scotopic and photopic responses in ciliary neurotrophic factor-treated retinas[42] has led to the evaluation of other trophic factors such as glial cell derived neurotrophic factor.[12,43,44] In addressing the secondary degeneration of cones, RdCVF administration may be used to target a pathological mechanism common to most forms of the disease. The retinal cone cells are responsible for all visual functions in normal light. Therefore, preventing their degeneration is a rational strategy in the treatment of RP patients. This objective is medically feasible because 50% cone loss does not result in significant loss of visual acuity,[5] and it has been estimated that this approach may prevent up to 1.5 million people worldwide from becoming blind.[6]

The present study on the P23H rat suggests that RdCVF administration may be efficient in the treatment of autosomal dominant RP due to rhodopsin mutations, which account for 30–40% of cases of human autosomal dominant RP (http://www.sph.uth.tmc.edu/Retnet/). However, photoreceptor transplantation is limited by the availability of the donors and the potential risks of contamination.[45] Also, the clinical importance of RdCVF is further suggested by the existence of RdCVF variants associated with Leber congenital amaurosis.[46] Several issues need to be addressed for us to translate our observation of functional rescue of cones by subretinal administration of RdCVF to the point of evaluation in a clinical trial. Different modes of protein delivery are indeed currently used for retinal diseases: repeated intravitreal injections as for antivascular endothelial growth factor therapy in age-related macular degeneration[47] or intravitreal implants containing engineered cells producing the proteins.[48] In both cases, the protein achieves its effect on the outer retina via delivery to the vitreous. Further studies will assess the dose–response curve of RdCVF injection on cone survival in P23H rats and evaluate whether vitreal administrations in large animal models (*e.g., rcd1* dog) could also lead to a similar functional rescue of cones. These detailed studies will address the questions of pharmacokinetics of the protein. In the alternative, RdCVF protein might be delivered using adeno-associated virus vectors.[49,50] A positive result would then open the way for RdCVF clinical validation and bring much hope to patients suffering from RP, a strategy that may be applicable to a majority of RP mutations, with relevance even at late stages of the disease when rods have already disappeared and can no longer be rescued.

MATERIALS AND METHODS

Animals. Experimental procedures adhered to the Association for Research in Vision and Ophthalmology Statement for the Use of Animals in Ophthalmology and Vision Research. Transgenic homozygous P23H rats (line 1) were kindly provided by Matthew LaVail, PhD (UCSF School of Medicine, Beckman Vision Center) and were crossed with albino Sprague-Dawley rats to obtain heterozygous animals that were used in all experiments. All animals were bred and maintained under a 12-hour light/dark cycle with a room illumination of around 15 lux at 25 °C. They were housed with the authorization and supervision of the institutional Animal Care from INSERM UMR592. The animals were divided into two groups, and operations were performed by randomly selecting the eye to be treated. The unoperated eye from each rat was considered as natural control (contralateral controls): group 1: ten 3-month-old rats for phosphate buffered saline subretinal injection—sham controls (SM) and group 2: fifteen 6-month-old rats for RdCVF injection (RdCVF). ERG recordings have been performed for each animal after surgery at the age of 9 months. The animals were sacrificed with overdose anesthesia: 2–2.5 ml ketamine 500 (Rhone Merieux, Lyon, France).

Data mining. A PSI-BLAST (position-specific, iterative, basic local alignment search tool) of mouse peptide was performed on EST databank from *Rattus norvegicus*. One EST (BE108041) was found to 443 pb mRNA homologous sequence in the reverse orientation (3′→5′). This EST was then localized in genomic sequence from *Rattus norvegicus* (contig: ac122603). The first exon of the gene was located between position 88,325 and 88,654 and the second from position 89,977 to 90,304. A stop codon in frame within the first intron immediately following the exon 1 predicts the production of a truncated form of the thioredoxin-like six protein as observed for mouse. Full-length open-reading frame corresponding to the rat RdCVF sequence was amplified by RT-PCR from normal rat retina and the resulting product sequenced. The 330 pb sequence is identical to that of the rat RdCVF gene mined in the genomic database (**Figure 2a**). Rat RdCVF is 98% homologous to RdCVF from mouse (**Figure 2b**). There are two conservative changes in amino acid sequences: V2A and D106E.

RT–PCR analysis. Retinal total RNA from Sprague-Dawley and transgenic rats was purified using CsCl centrifugation and reverse transcribed into cDNAs by random hexamers (pdN_6) according to standard protocols. First strand cDNA (0.25 μl) was amplified using 1 μmol/l of sequence-specific primers on a LightCycler instrument (Roche-Diagnostics, Indianapolis, IN) and with SYBR Green I (LightCycler Faststart DNA Master^{PLUS} SYBR Green I), according to the manufacturer's recommendations. Cycling conditions were as follows: initial denaturation at 95 °C for 1 minute, following by 40 cycles of denaturation at 95 °C for 0 second, annealing at 57 °C for 5 seconds, elongation at 72 °C for 13 seconds ended by a gradual increase (0.1 °C/second) in temperature to 95 °C. Real-time PCR efficiencies were evaluated by calculating the slope of a linear regression graph. For each experiment, crossing points were calculated by the LightCycler Data Analysis Program (LightCycler-3.5 Software). Gene expression levels were normalized with respect to that of β-actin.

© The American Society of Gene Therapy

The oligonucleotides used were: 5′-AGCACAAGACGATTCTCTAAC-3′, 5′-AACCCTCTCTCAAAACCAAAC-3′ for RdCVF total (141 bp both short and long isoforms of the messenger RNA), 5′-TACAGAGG AGCAACAGGACCTGTTCCTCCGG-3′, 5′-CGTCAACTGCCAGCGG TCGTGGTACTCAA-3′ for RdCVF-L (130 bp); 5′-TTCCTGCCGTT CCATGATGACC-3′, 5′-TAGCAATCCTCCTGTCTTCCCTCC-3′ for RdCVF (227 bp). Results are represented in percentage compared to β-actin (296 bp) expression for which level is 100%.

RdCVF injection. Human RdCVF polypeptide (109 amino acids) was synthesized at GeneProt (Geneva, Switzerland) and refolded (>90% purity). The protective effect of the RdCVF synthetic protein on cone-enriched cultures from chicken embryos was performed as previously described.[11] The injections were performed totally three times and monthly—at different postnatal months (6, 7, and 8 months). Before injections, rats were anesthetized by intramuscular injection of a mixture of ketamine (100 mg/kg) and xylazine (10 mg/kg). After anesthetizing, we exposed the superior sclera and performed a small hole by using a 10-0 needle. The induction of a local retinal detachment was checked in order to confirm the success of the subretinal injection procedure. The local retinal detachment was chosen at different locations to maximize delivery. The microsyringe (10 µl; Hamilton, Reno, NY) was then gently inserted into the subretinal space, and 3 µl of synthetic RdCVF protein (concentration: 0.5 µg/µl) was injected. We used the same procedure for sham surgery where only phosphate buffered saline was injected to the control eye.

Cell counts and measurement of the tip areas of cone outer segments. The total numbers of peanut agglutinin lectin-labeled cones were estimated in the flat-mounted retinas by using a stereological counting approach to achieve unbiased sampling as previously described.[9] The rat retina was subdivided into 225 fields representing a surface of 1,225 µm^2 each. A zone of 2 mm radius center on the optic nerve was omitted in the counting. Approximately 120–200 fields distributed throughout the remaining whole retinal surface were chosen for cone counting by using a systematic random sampling procedure: an initial random choice was made for the first measurement, and all subsequent sampling was performed at predetermined intervals throughout the retinal surface. Each field was observed and the number of cone visually counted by using a Nikon Plan ×40 objective on a Nikon photomicroscope equipped with a Sony Trinitron color graphic display camera (Sony, Tokyo, Japan). The counted cone numbers and fields were cumulated automatically by the computer during the counting. The average of cone number per field was calculated in order to estimate the number of cone photoreceptors per millimeter square. The cone counts were expressed as density over the estimated retinal surface.

To measure the tip areas of cone outer segments, the flat-mounted retinas were scanned by automated acquisition system, using a Nikon Plan ×40 objective. We chose five retinas of each group from RdCVF-treated, control, and sham groups and 40 fields of each retina at 2 mm away from their optic disc in all directions. The areas of 5–25 cones in each field were measured in a masked analysis, by pixels ($X = Y = 1$ pixel = 0.3225 µm). The tip areas of peanut agglutinin lectin labeling were calculated and shown as **Figure 5i**. In order to get more details from the morphology of the cones, the images built from nine focus plans were reconstructed in 3D using Metamorph software and converted into 2D using the optimal focus.

ERG recordings. Following overnight dark adaptation, animals were prepared for recording under dim red light. After intramuscular anesthesia with a mixture of ketamine (100 mg/kg) and xylazine (10 mg/kg), pupils were dilated with 0.5% tropicamide or 1% atropine, and the cornea was locally anesthetized with oxbuprocaine application. Upper and lower lids were retracted to keep the eye open and proptosed. Body temperature was maintained at ~37 °C with a heating pad. A gold-loop electrode was placed on the corneal surface and maintained with lacrigel (Europhta, Monaco). A stainless-steel reference electrode was inserted subcutaneously on the head of the rat and a second needle electrode inserted subcutaneously in the back of the rat served to ground the signal. The light stimulus was provided by a 150-W xenon lamp in a Ganzfeld stimulator (Multiliner Vision; Jaeger/Toennies, Hochberg, Germany), increasing from –4 to 1.4 log candela (cd)/m^2. Photopic cone ERGs were performed on a rod-suppressing background after 5-minute light adaptation. The duration of the light stimulus was constant. Responses were amplified and filtered (1 Hz-low and 300 Hz-high cutoff filters) with a 1-channel DC-/AC-amplifier. Within each treatment group, ERG recordings were performed on separate days between the treated and the control eyes in order to prevent interference of stimulations between the two eyes of the same animal. Each scotopic or photopic ERG response represents the average of five responses from a set of five flashes of stimulation. To avoid corneal opacity for the unrecorded eye during the operation, a drop of lacrigel was applied, covering the surface of cornea, and the eyelids were closed by tweezers.

Statistical analysis. We used Smirnov's method to distinguish whether the data followed a normal distribution. As we selected randomly one eye of each rat for the treated sample, and another eye for the control in all the experiment groups, all the samples for ERG and cell counts were paired to compare treated versus control retinas in each group (cone number of each mm^2 per retina; amplitude and latency of ERG A and B waves separately). Student's *t*-test was performed for paired series—ERG and cell counts. Analysis of variance and *t*-test were used for unpaired series—the size of the tip areas of cone outer segments.

SUPPLEMENTARY MATERIAL

Figure S1. Morphology of cones in the RdCVF untreated and treated retinas.

Table S1. RdCVF injection: photopic B-wave amplitudes and cone counts of the RdCVF protein injected and contralateral controls eyes from P23H rats.

Table S2. Sham operation: photopic B-wave amplitudes and cone counts of the PBS injected eyes from P23H rats.

Materials and Methods.

ACKNOWLEDGMENTS

We thank Frédéric Chalmel and Olivier Poch for their contribution to the bioinformatic analysis (IGBMC); George Lambrou, Valérie Heidinger, and Anne-Ulrike Trendelenburg for providing synthetic RdCVF protein (Novatris Ophthamics); Matthew Lavail for generously providing the P23H rat line and for his collaboration in studying cone cell degeneration in this model; Géradine Millet-Puel, Marie-Laure Niepon, and Najate Aït-Ali for technical help; Thérèse Cronin for reading the manuscript and Stephane Fouquet for confocal microscope technique supports. This work was supported by INSERM, EVI-GENORET, and Foundation Fighting Blindness (USA).

REFERENCES

1. Hartong, DT, Berson, EL and Dryja, TP (2006). Retinitis pigmentosa. *Lancet* **18**: 1795–1809.
2. Rosenfeld, PJ, Cowley, GS, McGee, TL, Sandberg, MA, Berson, EL and Dryja, TP (1992). A null mutation in the rhodopsin gene causes rod photoreceptor dysfunction and autosomal recessive retinitis pigmentosa. *Nat Genet* **1**: 209–213.
3. McLaughlin, ME, Sandberg, MA, Berson, EL and Dryja, TP (1993). Recessive mutations in the gene encoding the beta-subunit of rod phosphodiesterase in patients with retinitis pigmentosa. *Nat Genet* **4**: 130–134.
4. Mangel, SC and Dowling, JE (1987). The interplexiform-horizontal cell system of the fish retina: effects of dopamine, light stimulation and time in the dark. *Proc R Soc Lond B Biol Sci* **22**: 91–121.
5. Geller, AM and Sieving, PA (1993). Assessment of foveal cone photoreceptors in Stargardt's macular dystrophy using a small dot detection task. *Vision Res* **33**: 1509–1524.
6. Wright, AF (1997). A searchlight through the fog. *Nat Genet* **17**: 132–134.
7. Mohand-Said, S, Hicks, D, Dreyfus, H and Sahel, JA (2000). Selective transplantation of rods delays cone loss in a retinitis pigmentosa model. *Arch Ophthalmol* **118**: 807–811.
8. Mohand-Said, S, Hicks, D, Simonutti, M, Tran-Minh, D, Deudon-Combe, A, Dreyfus, H *et al.* (1997). Photoreceptor transplants increase host cone survival in the retinal degeneration (rd) mouse. *Ophthalmic Res* **29**: 290–297.
9. Mohand-Said, S, Deudon-Combe, A, Hicks, D, Simonutti, M, Forster, V, Fintz, AC *et al.* (1998). Normal retina releases a diffusible factor stimulating cone survival in the retinal degeneration mouse. *Proc Natl Acad Sci USA* **95**: 8357–8362.

© The American Society of Gene Therapy

10. Fintz, AC, Audo, I, Hicks, D, Mohand-Said, S, Léveillard, T and Sahel, J (2003). Partial characterization of retina-derived cone neuroprotection in two culture models of photoreceptor degeneration. *Invest Ophthalmol Vis Sci* **44**: 818–825.
11. Léveillard, T, Mohand-Saïd, S, Lorentz, O, Hicks, D, Fintz, AC, Clérin, E *et al.* (2004). Identification and characterization of rod-derived cone viability factor. *Nat Genet* **36**: 755–759.
12. Frasson, M, Picaud, S, Léveillard, T, Simonutti, M, Mohand-Said, S, Dreyfus, H *et al.* (1999). Glial cell line-derived neurotrophic factor induces histologic and functional protection of rod photoreceptors in the rd/rd mouse. *Invest Ophthalmol Vis Sci* **40**: 2724–2734.
13. Bowes, C, Li, T, Danciger, M, Baxter, LC, Applebury, ML and Farber, DB (1990). Retinal degeneration in the rd mouse is caused by a defect in the beta subunit of rod cGMP-phosphodiesterase. *Nature* **347**: 677–680.
14. Cronin, T, Léveillard, T and Sahel, JA (2007). Retinal degenerations: from cell signaling to cell therapy; pre-clinical and clinical issues. *Curr Gene Ther* **7**: 121–129.
15. Wen, R, Song, Y, Kjellstrom, S, Tanikawa, A, Liu, Y, Li, Y *et al.* (2006). Regulation of rod phototransduction machinery by ciliary neurotrophic factor. *J Neurosci* **26**: 13523–13530.
16. Sieving, PA, Caruso, RC, Tao, W, Coleman, HR, Thompson, DJ, Fullmer, KR *et al.* (2006). Ciliary neurotrophic factor (CNTF) for human retinal degeneration: phase I trial of CNTF delivered by encapsulated cell intraocular implants. *Proc Natl Acad Sci USA* **103**: 3896–3901.
17. Lee, D, Geller, S, Walsh, N, Valter, K, Yasumura, D, Matthes, M *et al.* (2003). Photoreceptor degeneration in Pro23His and S334ter transgenic rats. *Adv Exp Med Biol* **533**: 297–302.
18. Machida, S, Kondo, M, Jamison, JA, Khan, NW, Kononen, LT, Sugawara, T *et al.* (2000). P23H rhodopsin transgenic rat: correlation of retinal function with histopathology. *Invest Ophthalmol Vis Sci* **41**: 3200–3209.
19. Carter-Dawson, LD, LaVail, MM and Sidman, RL (1978). Differential effect of the rd mutation on rods and cones in the mouse retina. *Invest Ophthalmol Vis Sci* **17**: 489–498.
20. Chalmel, F, Léveillard, T, Jaillard, C, Lardenois, A, Berdugo, N, Morel, E *et al.* (2007). Rod-derived Cone Viability Factor-2 is a novel bifunctional-thioredoxin-like protein with therapeutic potential. *BMC Mol Biol* **8**: 74.
21. Aizawa, S, Mitamura, Y, Baba, T, Hagiwara, A, Ogata, K and Yamamoto, S (2009). Correlation between retinal sensitivity and photoreceptor inner/outer segment junction in patients with retinitis pigmentosa. *Br J Ophthalmol* **93**: 126–127.
22. Punzo, C, Kornacker, K and Cepko, CL (2009). Stimulation of the insulin/mTOR pathway delays cone death in a mouse model of retinitis pigmentosa. *Nat Neurosci* **12**: 44–52.
23. Dryja, TP, McGee, TL, Reichel, E, Hahn, LB, Cowley, GS, Yandell, DW *et al.* (1990). A point mutation of the rhodopsin gene in one form of retinitis pigmentosa. *Nature* **343**: 364–366.
24. Petters, RM, Alexander, CA, Wells, KD, Collins, EB, Sommer, JR, Blanton, MR *et al.* (1997). Genetically engineered large animal model for studying cone photoreceptor survival and degeneration in retinitis pigmentosa. *Nat Biotechnol* **15**: 965–970.
25. Naash, MI, Hollyfield, JG, al-Ubaidi, MR and Baehr, W (1993). Simulation of human autosomal dominant retinitis pigmentosa in transgenic mice expressing a mutated murine opsin gene. *Proc Natl Acad Sci USA* **90**: 5499–5503.
26. Goto, Y, Peachey, NS, Ripps, H and Naash, MI (1995). Functional abnormalities in transgenic mice expressing a mutant rhodopsin gene. *Invest Ophthalmol Vis Sci* **36**: 62–71.
27. McCall, MA, Gregg, RG, Merriman, K, Goto, Y, Peachey, NS and Stanford, LR (1996). Morphological and physiological consequences of the selective elimination of rod photoreceptors in transgenic mice. *Exp Eye Res* **63**: 35–50.
28. Hewitt, AT, Lindsey, JD, Carbott, D and Adler, R (1990). Photoreceptor survival-promoting activity in interphotoreceptor matrix preparations: characterization and partial purification. *Exp Eye Res* **50**: 79–88.
29. Huang, PC, Gaitan, AE, Hao, Y, Petters, RM and Wong, F (1993). Cellular interactions implicated in the mechanism of photoreceptor degeneration in transgenic mice expressing a mutant rhodopsin gene. *Proc Natl Acad Sci USA* **90**: 8484–8488.
30. Kedzierski, W, Bok, D and Travis, GH (1998). Non-cell-autonomous photoreceptor degeneration in rds mutant mice mosaic for expression of a rescue transgene. *J Neurosci* **18**: 4076–4082.
31. Goldsmith, P, Baier, H and Harris, WA (2003). Two zebrafish mutants, ebony and ivory, uncover benefits of neighborhood on photoreceptor survival. *J Neurobiol* **57**: 235–245.
32. Portera-Cailliau, C, Sung, CH, Nathans, J and Adler, R (1994). Apoptotic photoreceptor cell death in mouse models of retinitis pigmentosa. *Proc Natl Acad Sci USA* **1**: 974–978.
33. Lolley, RN, Rayborn, ME, Hollyfield, JG and Farber, DB (1980). Cyclic GMP and visual cell degeneration in the inherited disorder of rd mice: a progress report. *Vision Res* **20**: 1157–1161.
34. Vallazza-Deschamps, G, Cia, D, Gong, J, Jellali, A, Duboc, A, Forster, V *et al.* (2005). Excessive activation of cyclic nucleotide-gated channels contributes to neuronal degeneration of photoreceptors. *Eur J Neurosci* **22**: 1013–1022.
35. Sanges, D, Comitato, A, Tammaro, R and Marigo, V (2006). Apoptosis in retinal degeneration involves cross-talk between apoptosis-inducing factor (AIF) and caspase-12 and is blocked by calpain inhibitors. *Proc Natl Acad Sci USA* **14**: 17366–17371.
36. Gorbatyuk, M, Justilien, V, Liu, J, Hauswirth, WW and Lewin, AS (2007). Suppression of mouse rhodopsin expression *in vivo* by AAV mediated siRNA delivery. *Vision Res* **47**: 1202–1208.
37. Chrysostomou, V, Stone, J, Stowe, S, Barnett, NL and Valter, K (2008). The status of cones in the rhodopsin mutant P23H-3 retina: light-regulated damage and repair in parallel with rods. *Invest Ophthalmol Vis Sci* **49**: 1116–1125.
38. Wang, XW, Tan, BZ, Sun, M, Ho, B and Ding, JL (2008). Thioredoxin-like 6 protects retinal cell line from photooxidative damage by upregulating NF-kappaB activity. *Free Radic Biol Med* **45**: 336–344.
39. Steinberg, RH, Fisher, SK and Anderson, DH (1980). Disc morphogenesis in vertebrate photoreceptors. *J Comp Neurol* **190**: 501–508.
40. Delyfer, MN, Léveillard, T, Mohand-Said, S, Hicks, D, Picaud, S and Sahel, JA (2004). Inherited retinal degenerations: therapeutic prospects. *Biol Cell* **96**: 261–269.
41. Faktorovich, EG, Steinberg, RH, Yasumura, D, Matthes, MT and LaVail, MM (1990). Photoreceptor degeneration in inherited retinal dystrophy delayed by basic fibroblast growth factor. *Nature* **347**: 83–86.
42. Rhee, KD, Ruiz, A, Duncan, JL, Hauswirth, WW, LaVail, MM, Bok, D *et al.* (2007). Molecular and cellular alterations induced by sustained expression of ciliary neurotrophic factor in a mouse model of retinitis pigmentosa. *Invest Ophthalmol Vis Sci* **48**: 1389–1400.
43. McGee Sanftner, LH, Abel, H, Hauswirth, WW and Flannery, JG (2001). Glial cell line derived neurotrophic factor delays photoreceptor degeneration in a transgenic rat model of retinitis pigmentosa. *Mol Ther* **4**: 622–629.
44. Buch, PK, Maclaren, RE, Duran, Y, Balaggan, KS, MacNeil, A, Schlichtenbrede, FC *et al.* (2006). In contrast to AAV-mediated Cntf expression, AAV-mediated Gdnf expression enhances gene replacement therapy in rodent models of retinal degeneration. *Mol Ther* **14**: 700–709.
45. Chong, NH and Bird, AC (1999). Management of inherited outer retinal dystrophies: present and future. *Br J Ophthalmol* **83**: 120–122.
46. Hanein, S, Perrault, I, Gerber, S, Dollfus, H, Dufier, JL, Feingold, J *et al.* (2006). Disease-associated variants of the rod-derived cone viability factor (RdCVF) in Leber congenital amaurosis. Rod-derived cone viability variants in LCA. *Adv Exp Med Biol* **572**: 9–14.
47. Rosenfeld, PJ, Brown, DM, Heier, JS, Boyer, DS, Kaiser, PK, Chung, CY *et al.* (2006). Ranibizumab for neovascular age-related macular degeneration. *N Engl J Med* **5**: 1419–1431.
48. Tao, W (2006). Application of encapsulated cell technology for retinal degenerative diseases. *Expert Opin Biol Ther* **6**: 717–726.
49. Maguire, AM, Simonelli, F, Pierce, EA, Pugh, EN Jr, Mingozzi, F, Bennicelli, J *et al.* (2008). Safety and efficacy of gene transfer for Leber's congenital amaurosis. *N Engl J Med* **358**: 2240–2248.
50. Bainbridge, JW, Smith, AJ, Barker, SS, Robbie, S, Henderson, R, Balaggan, K *et al.* (2008). Effect of gene therapy on visual function in Leber's congenital amaurosis. *N Engl J Med* **358**: 2231–2239.